Journal of Experimental Marine Biology and Ecology 406 (2011) 38–45

Contents lists available at ScienceDirect

Journal of Experimental Marine Biology and Ecology

journal homepage: www.elsevier.com/locate/jembe

Neither elevated nor reduced CO_2 affects the photophysiological performance of the marine Antarctic diatom *Chaetoceros brevis*

Peter Boelen [a,*], Willem H. van de Poll [a], Han J. van der Strate [a], Ika A. Neven [b], John Beardall [c], Anita G.J. Buma [a]

[a] Department of Ocean Ecosystems, ESRIG, University of Groningen, P.O. Box 11103, 9700 CC Groningen, The Netherlands
[b] Department of Plant Physiology, CEES, University of Groningen, P.O. Box 11103, 9700 CC Groningen, The Netherlands
[c] School of Biological Sciences, Monash University, Clayton, Victoria 3800, Australia

ARTICLE INFO

Article history:
Received 9 February 2011
Received in revised form 8 June 2011
Accepted 9 June 2011
Available online xxxx

Keywords:
Climate change
Dynamic irradiance
Phytoplankton
Southern Ocean
Vertical mixing
Xanthophyll cycling

ABSTRACT

Enhanced or reduced pCO_2 (partial pressure of CO_2) may affect the photosynthetic performance of marine microalgae since changes in pCO_2 can influence the activity of carbon concentrating mechanisms, modulate cellular RuBisCO levels or alter carbon uptake efficiency. In the present study we compared the photophysiology of the Antarctic diatom *Chaetoceros brevis* at two pCO_2 extremes: 750 ppmv (2× ambient) and 190 ppmv (0.5× ambient) CO_2. Cultures were acclimated to four irradiance regimes: two regimes simulating deep or shallow vertical mixing, and two regimes mimicking limiting and saturating stable water column conditions. Then, growth rate, pigmentation, RuBisCO large subunit expression, RuBisCO activity, photosynthesis vs irradiance curves, effective quantum yield of PSII (F_v/F_m), and POC were measured.
The four irradiance regimes induced a suite of photophysiological responses, ranging from low light acclimation to efficient photoprotection. Growth was reduced under the low constant and the deep mixing regime, compared to the shallow mixing and the stable saturating regime. Low stable irradiance resulted in higher light harvesting pigment concentrations, lower RuBisCO activity and a lower light saturation point (E_k) compared to the other irradiance regimes. Highest RuBisCO activity as well as P_{max} levels was measured in the shallow mixing regime, which received the highest total daily light dose. Photoprotection by xanthophyll cycling was observed under all irradiance regimes except the low stable irradiance regime, and xanthophyll cycle pool sizes were higher under the dynamic irradiance regimes. For the fluctuating irradiance regimes, F_v/F_m was hardly affected by previous excess irradiance exposure, suggesting minimal PSII damage. No significant differences between the two pCO_2 levels were found, with respect to growth, pigment content and composition, photosynthesis, photoprotection and RuBisCO activity, for all four irradiance regimes. Thus, within the range tested, pCO_2 does not significantly affect the photophysiological performance of *C. brevis*.

1. Introduction

In nearly all phototrophic microorganisms, including marine phytoplankton, CO_2 is fixed by the carboxylating enzyme ribulose-1,5-bisphosphate carboxylase/oxygenase (RuBisCO). Since the half saturation constant of RuBisCO for CO_2 is much higher than present-day CO_2 concentrations in seawater (Badger et al., 1998), algae have developed mechanisms to increase intracellular CO_2 concentrations. These carbon concentrating mechanisms (CCMs) elevate the steady state CO_2 concentration around RuBisCO by active transport of inorganic carbon across the cell membrane. Mechanisms to elevate intracellular CO_2 concentration are believed to be energetically costly because many marine phytoplankton species down-regulate CCM capacity under increased pCO_2 (partial pressure of CO_2) (Beardall and Giordano, 2002). Trimborn et al. (2009) studied the effect of pCO_2 on carbon acquisition and intracellular assimilation in bloom forming and non-bloom-forming diatom species. Inorganic carbon uptake kinetics and extracellular carbonic anhydrase activities were highly regulated in the bloom-forming diatom species while the non-bloom-forming species displayed an efficient but not regulated CCM. Since pCO_2 levels in the surface of the ocean are predicted to double over their present values by the middle of this century (IPCC, 2007), it might be expected that the capacity to down-regulate a CCM will form a significant competitive advantage in the future. Indeed, for some phytoplankton species an increase in growth rate was demonstrated under elevated pCO_2 (Clark and Flynn, 2000; Beardall and Raven, 2004 and references therein). However, contrasting results were found for growth rates of other species that were not or only slightly affected by enhanced CO_2 (e.g. Burkhardt et al., 1999).

* Corresponding author. Tel.: +31 503636140; fax: +31 503632261.
E-mail address: p.boelen@rug.nl (P. Boelen).

0022-0981/$ – see front matter © 2011 Elsevier B.V. All rights reserved.
doi:10.1016/j.jembe.2011.06.012

Many laboratory experiments apply constant levels of saturating irradiance, providing the algae with enough energy to maintain efficient CCMs. This contrasts with field conditions where light is frequently limiting photosynthesis and highly variable. Prevailing strong winds can induce deep wind mixed layers, particularly in the cold non stratified waters of the Southern Ocean (Nelson and Smith, 1991). Therefore, incident irradiance is believed to limit primary production in the Southern Ocean (Sakshaug et al., 1991). Deep vertical mixing reduces daily irradiance doses, whereas constant regulation of photosynthesis and carboxylase activity is needed to cope with the fluctuating irradiance levels. Furthermore, Antarctic phytoplankton from deep mixed layers are sensitive to photoinhibition when exposed to near surface irradiance (Alderkamp et al., 2010). Photoprotection of phytoplankton depends strongly on the responses that are regulated on a short time scale (seconds, minutes) such as the xanthophyll cycle (enzymatically reversible conversion between epoxyxanthophyll and de-epoxyxanthophyll), that is driven by changes in pH in the thylakoid lumen (Olaizola et al., 1994). De-epoxidation of diadinoxanthin to diatoxanthin results in non photochemical quenching of chlorophyll fluorescence, which increases heat dissipation of excessively absorbed energy (Goss and Jakob, 2010). This process minimizes PSII repair after excess irradiance, thereby facilitating recovery of photosynthesis under favorable conditions (Moisan et al., 1998; van de Poll et al., 2007; van de Poll and Buma, 2009). Photoacclimation processes occur on longer time scales (hours to days) and include the adjustment of PSII reaction centers, pigment levels, RuBisCO activity and PSII repair. Yet, acclimation processes are likely not fast enough to maintain optimal photosynthetic capacity during mixing (MacIntyre et al., 2000; Moore et al., 2006).

CO_2 potentially affects photoacclimation, via the regulation of carbon concentrating mechanisms or modulation of cellular RuBisCO levels (Reinfelder, 2011; Tortell et al., 2000). Apart from this, elevated pCO_2 can increase the efficiency of carbon uptake, and thereby increase the capacity of the RuBisCO electron sink. We hypothesized that elevated pCO_2 could therefore expand the irradiance range that supports growth in phytoplankton, thereby reducing the requirement for photoprotection from the xanthophyll cycle. In contrast, low pCO_2 would reduce the irradiance range that supports growth and consequently increases the demand for photoprotection. Such changes would affect phytoplankton photosynthesis under stable and non stable water column conditions.

In the present study we investigated the impact of pCO_2 on a range of photophysiological responses in the Antarctic diatom *Chaetoceros brevis*. Cultures were exposed to two pCO_2 extremes: 750 ppmv (2× ambient) and 190 ppmv (0.5× ambient) CO_2 and four highly different irradiance regimes: two regimes simulating deep or shallow vertical mixing, and two regimes mimicking limiting and saturating stable water column conditions. After acclimation, growth, carbon and pigment content, PSII efficiency, photosynthetic O_2 evolution as well as carboxylase (RuBisCO) activity and the gene expression of the large RuBisCO subunit were quantified.

2. Materials and methods

2.1. Experimental set-up

Cultures of the Antarctic microalga *C. brevis* (Bacillariophyceae; CCMP163) were grown at 4 °C in f/2 enriched (Guillard and Ryther, 1962) filter-sterilized seawater adjusted to a salinity of 35‰. Two series of experiments were performed.

2.1.1. Stability of the sea water carbonate system

In order to check if CO_2 conditions were stable over the time course of the experiments, the sea water carbonate system was first investigated in response to *C. brevis* growth. One liter vessels were continuously aerated with filtered synthetic air containing 190 and 750 ppmv CO_2 (Linde Gas, Schiedam, The Netherlands) at a flow rate of 7 L h^{-1}. The synthetic air first entered a 1 L vessel with seawater to humidify the air, preventing evaporation, before entering the culture vessel. The experiment was started with an initial concentration of ~$1*10^4$ cells mL^{-1} from a *C. brevis* stock culture that was growing under the same conditions for a week. The cultures were illuminated with three 30 W Osram Biolux fluorescent lamps providing 70 µmol photons m^{-2} s^{-1}, following a 16:8 h light:dark cycle, at 4.5 °C. During this experiment (7 days of exponential growth) cell concentrations (see below), pH (NBS scale, Metrohm 780 pH meter) and dissolved inorganic carbon (DIC) was monitored. For DIC, 12 mL samples were fixed with 3 µL of a saturated aqueous solution of $HgCl_2$ (DOE, 1994) in glass tubes with vacuum greased caps. Samples were stored cold (4 °C) and dark until analysis (see below). The parameters of the seawater carbonate system were calculated from pH, DIC, silicate, phosphate, temperature and salinity using the program CO2sys (Lewis and Wallace, 1998) (with the equilibrium constants of Mehrbach et al. (1973) refitted by Dickson and Millero, 1987). The experiment was terminated at cell concentrations of $1.1*10^6$ and $6.9*10^5$ cells mL^{-1} for the 190 and 750 ppmv culture, respectively. There were no replicates in this experiment.

2.1.2. Responses to different pCO_2 and irradiance regimes

In the second series of experiments stock cultures were acclimated for at least 2 weeks to the four irradiance regimes (as described below) in a semi-continuous mode, without controlled pCO_2. Then, stock cultures were transferred to the culture vessels (1 L) at an initial cell density of circa $1*10^4$ cells mL^{-1} and continuously aerated with 0.2 µm filtered synthetic air containing 190 or 750 ppmv CO_2. These two CO_2 conditions (resp. 0.5× and 2× ambient (380 ppmv) CO_2) were chosen to represent low CO_2 (as observed during the last glacial maximum past and sometimes during large algal blooms) and high CO_2 (IPCC scenario predicted for the year 2100). The culture vessels were placed back in a PAR transmissive water bath (4 °C) placed inside a U-shape lamp setup as described by van de Poll et al. (2007). Twelve fluorescent lamps (six Biolux and six skywhite lamps, Osram) were connected to dimmers and computer-controlled by LabView (National Instruments) software allowing irradiance fluctuations between 7 and 1222 µmol photons m^{-2} s^{-1}. Four different light regimes were studied. Two cultures were subjected to fluctuating irradiance regimes simulating deep (cyclic transport between 0 and 50 m depth, including transport below the photic zone; "mixed 50 m") or shallow (cyclic transport between 0 and 10 m depth; "mixed 10 m") vertical mixing. The third and fourth cultures were exposed to low constant irradiance (7 µmol photons m^{-2} s^{-1} following a 10:14 h light:dark cycle; "non-mixed 50 m") and a sinusoidal diurnal light cycle ("non-mixed 15 m") mimicking a stable water column (Fig. 1). Although the daily integral of irradiance (total daily light dose; TDLD) was similar for the "mixed 50 m" and the "non-mixed 15 m" irradiance regime (for both irradiance regimes circa 6.5 mol m^{-2} day^{-1}, Table 1), the "mixed 50 m" irradiance regime is potentially growth-limiting since periods of irradiance are short and intense (i.e. above saturating levels) and followed by dark periods, resulting in a relatively low daily integral of photosynthesis. Growth was followed during the exponential growth phase (7–16 days, depending on the irradiance conditions). Before the start and at the end of the experiment the pH (NBS scale) was determined. Measured pH values did not deviate more than 0.1 pH unit compared to cell-free medium values at the respective pCO_2 (8.43 ± 0.07 and 7.90 ± 0.04 for low and high CO_2, respectively). In mid-exponential growth (between 2.3 and $3.6*10^5$ cells mL^{-1}), carbon and pigment content, PSII efficiency, photosynthetic O_2 evolution (photosynthesis vs. irradiance response curves) as well as RuBisCO activity and gene expression were quantified. Samples for pigment analysis and PSII efficiency were collected 3–11 times during the day (depending on

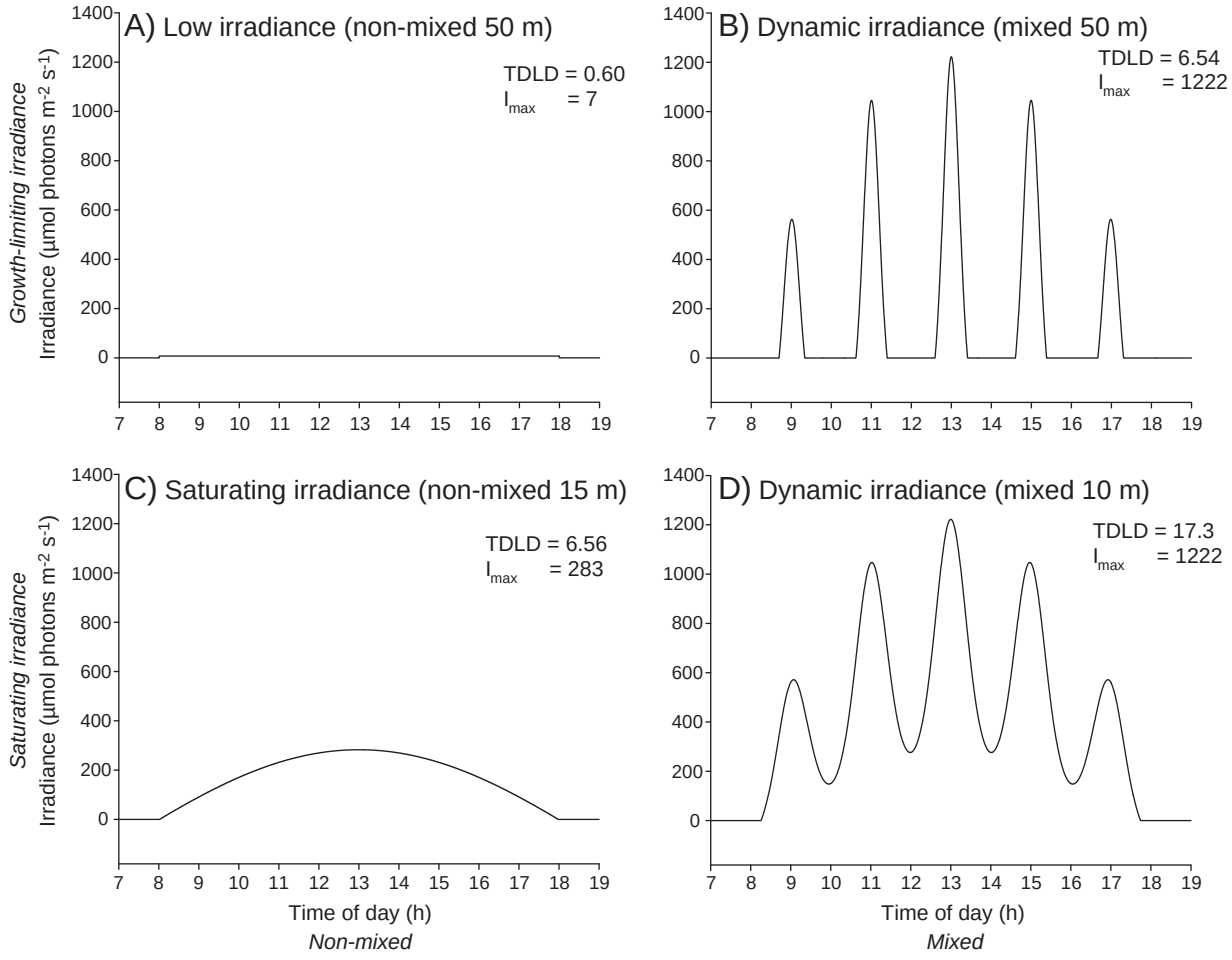

Fig. 1. Irradiance (µmol photons m^{-2} s^{-1}) during the four irradiance treatments. A) Growth-limiting low irradiance (non-mixed 50 m). B) Growth-limiting dynamic irradiance (mixed 50 m). C) Saturating irradiance (non-mixed 15 m). D) Saturating dynamic irradiance (mixed 10 m). Total daily light doses (TDLD; mol m^{-2} day^{-1}) and maximum irradiance levels (I_{max}; µmol m^{-2} s^{-1}) of the four irradiance treatments are plotted in the graphs.

irradiance dynamics). Samples for carbon content, photosynthesis vs. irradiance response curves, RuBisCO activity and RuBisCO gene expression were obtained before 8:00 h (dark) and at noon. The results shown are the averages based on two replicate cultures for each condition.

2.2. Analytical procedures

2.2.1. Cell counts

Cell numbers were determined using a Coulter XL-MCL flow cytometer (Beckman Coulter, Miami, FL, USA) as described by van de

Table 1
Specific growth rate, cellular carbon and pigment content, photosynthetic parameters (α, P_{max}, E_k; normalized to carbon), RuBisCO activity and gene expression (relative abundance of RuBisCO large subunit mRNA) of *C. brevis* grown at four irradiance conditions under low and high CO_2 (daily averages, mean value (±SD) of two independent experiments). Non-mixed 50 m; growth-limiting low irradiance. Mixed 50 m; growth-limiting dynamic irradiance. Non-mixed 15 m; saturating irradiance. Mixed 10 m; saturating dynamic irradiance.

Irradiance regime	Non-mixed 50 m		Mixed 50 m		Non-mixed 15 m		Mixed 10 m	
pCO_2	Low	High	Low	High	Low	High	Low	High
Specific growth rate (day^{-1})	0.209 (0.014)	0.209 (0.023)	0.200 (0.003)	0.216 (0.001)	0.477 (0.005)	0.483 (0.001)	0.447 (0.008)	0.451 (0.029)
Cellular carbon content (pg C $cell^{-1}$)	9.53 (0.19)	9.43 (0.35)	9.99 (0.61)	8.84 (1.44)	13.00 (0.23)	12.10 (0.98)	10.10 (1.04)	8.55 (0.97)
Light harvesting pigments: Chlorophyll *a* + Fucoxanthin (fg $cell^{-1}$)	623.74 (16.18)	591.48 (95.06)	411.18 (2.93)	386.64 (26.95)	272.66 (2.74)	273.50 (4.80)	309.85 (7.16)	305.86 (0.90)
Protective pigments: Diadinoxanthin + Diatoxanthin (fg $cell^{-1}$)	31.85 (0.04)	28.40 (6.63)	72.96 (2.18)	70.00 (6.19)	39.94 (6.55)	36.94 (0.99)	73.19 (3.34)	77.30 (2.88)
Initial slope of PE curve, α (mmol O_2 [g C]$^{-1}$ h^{-1} [µmol photons m^{-2} s^{-1}]$^{-1}$)	0.822 (0.138)	1.094 (0.437)	0.279 (0.018)	0.353 (0.015)	0.317 (0.034)	0.327 (0.058)	0.656 (0.045)	0.677 (0.062)
Maximum photosynthetic rate, P_{max} (mmol O_2 [g C]$^{-1}$ h^{-1})	9.23 (0.95)	11.81 (5.62)	10.52 (0.06)	9.95 (0.93)	9.57 (0.66)	10.84 (0.37)	17.20 (3.08)	18.64 (2.22)
Light saturation parameter, E_k (µmol photons m^{-2} s^{-1})	12.2 (0.2)	11.3 (0.5)	39.2 (3.5)	29.2 (1.5)	33.6 (7.2)	36.7 (2.5)	27.8 (4.3)	29.2 (1.6)
RuBisCO activity (mAbs340 mg protein^{-1} s^{-1})	2.08 (0.04)	3.70 (0.60)	11.86 (1.45)	12.20 (1.00)	10.74 (2.88)	10.73 (1.88)	15.38 (2.50)	14.06 (1.88)
Relative RuBisCO gene expression (au)	10.28 (7.23)	9.56 (9.30)	21.79 (1.59)	20.23 (12.64)	17.15 (0.88)	31.26 (0.25)	26.23 (0.68)	26.76 (6.71)

Poll et al. (2005). Average growth rates were calculated from linear regressions of the natural log of cell numbers versus time during 5 or more points in exponential growth.

2.2.2. Dissolved inorganic carbon (DIC)

DIC in samples from the first experiment was determined within 10 days using the following method: 0.3 mL sample was injected with a gastight Hamilton precision syringe through the septum of a glass vial containing 5 mL of 6 N HCl. Subsequently, all DIC was purged out by bubbling the sample with CO_2-free air at a known rate (mass flow controller, Brooks). After the removal of water vapor with a SiO_2 scrubber, CO_2 was measured with a Licor CO_2/H_2O gas analyzer (LI-7000). Concentrations were calculated from standard calibration curves with known amounts of $NaHCO_3$.

2.2.3. Elemental composition (POC and PON)

Particulate carbon (POC) and nitrogen were analyzed on a CHNS elemental analyzer type EA 1110 (Interscience) after gentle filtration (<15 kPa) of 15 mL samples over pre-combusted GF/F Whatman filters.

2.2.4. Pigment composition

Samples (30 mL) for pigment composition were filtered through GF/F (25 mm), immediately frozen in liquid nitrogen and stored at −80 °C until further analysis. The filters were freeze-dried (48 h) and extracted in 90% acetone (v/v, 48 h at 4 °C). Pigments were separated and quantified on a Waters HPLC system (model 2690) equipped with a 996 photodiode array detector and a C_{18} 5 μm DeltaPak reverse-phase column as described by van Leeuwe et al. (2006).

2.2.5. Chlorophyll fluorescence

Chlorophyll fluorescence parameters were determined with a pulse amplitude modulated chlorophyll fluorometer (Water-PAM; Heinz Walz GmbH, Germany). Samples (5 mL) were placed in a custom-made cuvette (2×2 cm). Basal fluorescence (F_t) was measured under weak measuring light and maximal fluorescence (F_m) was determined after a saturating light pulse (0.8 s, 4000 μmol photons m^{-2} s^{-1}). The effective quantum yield (without dark adaptation) of Photosystem II (Φ_{PSII}) was calculated as $(F'_m - F_t)/F'_m$ (Maxwell and Johnson, 2000).

2.2.6. Photosynthesis vs. irradiance response (PE) curves

PE curves were obtained by monitoring net oxygen evolution rates with an Oxy-4 four channel oxygen meter (Presens GmbH, Regensburg, Germany) equipped with dipping probe mini-sensors. Samples (15 mL) were placed in a custom-made incubation chamber, placed in a water bath to maintain constant temperature (4 °C). The cells were illuminated with four 18 W Osram "Cool Daylight" fluorescent tubes connected to a dimmer to measure oxygen evolution rates at 10–11 different light intensities (between 5 and 250 μmol photons m^{-2} s^{-1}). Gross photosynthesis-irradiance data (normalized to carbon) were fitted according to the exponential model of Webb et al. (1974):

$$P = P_{max}\left[1 - e^{(-\alpha I / P_{max})}\right]$$

where P_{max} is the gross maximum rate of photosynthesis (mmol O_2 [g C]$^{-1}$ h^{-1}) and α (mmol O_2 [g C]$^{-1}$ h^{-1} [μmol photons m^{-2} s^{-1}]$^{-1}$) the initial slope of the PE curve. The saturation point for photosynthesis E_k (μmol photons m^{-2} s^{-1}) was calculated as P_{max}/α.

2.2.7. RuBisCO activity

RuBisCO enzyme activity was determined following the procedure of Gerard and Driscoll (1996). Samples (100 mL) were filtered over 2.0 μm pore-size polycarbonate filters (Osmonics), immediately frozen in liquid nitrogen and stored at −80 °C until further analysis. Crude enzyme extracts were prepared by transferring the filters to test tubes containing ice-cold extraction buffer (25 mmol L^{-1} $KHCO_3$, 20 mmol L^{-1} $MgCl_2$, 0.2 mmol L^{-1} EDTA, 5 mmol L^{-1} DTT, 0.1% Triton X100, 50 mmol L^{-1} HEPES-KOH, pH 8.0). The cells were disrupted by sonication after which the extracts were centrifuged for 15 min (20,000 g) at 4 °C. From the supernatants 50 μL was used for determining the protein content (Biorad Protein Assay) and 150 μL for the RuBisCO activity assay. The assay mixture (pH 8.0) contained 25 mmol L^{-1} $KHCO_3$, 20 mmol L^{-1} $MgCl_2$, 0.2 mmol L^{-1} EDTA, 5 mmol L^{-1} DTT, 50 mmol L^{-1} HEPES-KOH, 3 mmol L^{-1} ATP, 0.2 mmol L^{-1} NADH, 5 mmol L^{-1} phosphocreatine, 22 units of creatine phosphokinase, 9 units of glyceraldehyde-3-phosphate dehydrogenase and 18 units of 3-phosphoglyceric phosphokinase. The mixture was placed in Cary 3E UV/Vis spectrophotometer and after temperature equilibration to 20 °C the background oxidation of NADH (absorbance at 340 nm) was followed during several minutes. The reaction was started by adding 2 mmol L^{-1} (final concentration) ribulose-1,5-biphosphate and the time course of NADH oxidation was recorded by the decrease in absorbance of 340 nm. The background oxidation of NADH was subtracted from the measured enzyme activity which was expressed as declining absorbance per mg of total protein and second (mAbs340 mg protein^{-1} s^{-1}).

2.2.8. RuBisCO large subunit expression

RuBisCO gene expression was determined by quantitative real-time PCR of the large subunit of RuBisCO. 50 mL of *C. brevis* cells were filtered and RNA was isolated using TRIzol® Reagent (1 mL per sample) according to the manufacturer (Invitrogen™ Life Technologies, Carlsbad, CA). The isolated RNA was subsequently treated with DNase I (Amersham Bioscience, Buckinghamshire, UK). RNA concentrations and purity were determined on the Nanodrop ND-1000 spectrophotometer (NanoDrop Technologies, Wilmington, DE). First strand cDNA was synthesized from 65 ng of DNA-free RNA using 500 ng oligo (dT) 12, 18 primer and Superscript™ III H reverse transcriptase (Invitrogen Life Technologies, Carlsbad, CA). cDNA concentrations were also determined on the Nanodrop ND-1000 spectrophotometer. Based on an alignment of known algal RuBisCO large subunit sequences, primers for *C. brevis* were designed using the program Primer3 (Rozen and Skaletsky, 2000). The designed RuBisCO Forward (5′-AAAATGGGTTACTGGGATGCTTC-3′) and RuBisCO Reverse (5′-CAGCAGCTTCTACTGGATCTACACC-3′) primers were synthesized by Biolegio B.V. (Nijmegen, The Netherlands). Amplification with these primers resulted in the expected 101 bp fragment for *C. brevis*. Quantitative real-time PCR (qRT-PCR) was performed using an iCycler 1 (Biorad, Hercules, CA). cDNA amplification reactions were performed in triplicate for every sample in a final reaction mixture of 15 μL, containing 1 μL cDNA (10 ng μL^{-1}), 7.5 μL Power SYBR Green Master Mix (Applied Biosystems, Foster City, CA), 0.5 μL of both forward and reverse primer (20 μM), and 5.5 μL H_2O). The amplification reaction was executed as followed: 2 min at 50 °C and 10 min at 95 °C, followed by 40 cycles of 15 s at 95 °C, and 60 s at 60 °C. Melting curves, for excluding nonspecific PCR side products, were acquired by heating the products for 15 s at 95 °C, 1 min at 55 °C, subsequent quick heating to 60 °C, followed by a more steady heating to 95 °C with increments of 0.5 °C/10 s. PCR amplifications without template (solely H_2O) and RNA samples without treatment with reverse transcriptase were used as controls. Four cDNA dilutions (1, 10, 100 and 1000 ng) were used to estimate the efficiency in a validation experiment. Individual PCR efficiency was calculated (Ramakers et al., 2003) to by-pass the assumption that in all samples the PCR efficiency is constant. The triplicate PCR reactions per sample were averaged before performing the $2^{-\Delta C}$t method (Livak and Schmittgen, 2001). Relative quantification was presented as the fold in change in mRNA transcript level relative to the sample with the lowest amount of mRNA transcripts present.

2.3. Statistical analysis

Differences in growth, photosynthesis and carboxylase activity among groups (4 irradiance regimes and 2 pCO_2 levels) were tested for significance by multi-factor ANOVA and were considered non significant at $p>0.05$. When differences were not significant, data were pooled and tested for significance by single-factor ANOVA. Post-hoc tests (Tukey HSD) were performed to further specify differences.

3. Results

3.1. Stability of the sea water carbonate system

Despite the fact that *C. brevis* exhibited high growth rates during this experiment (>0.66 day^{-1}), pH and DIC measurements indicated that the seawater carbonate system was relatively stable up to $1.0*10^6$ cells mL^{-1} (Fig. 2A). Calculated pCO_2 values varied between 150 and 230 ppm for the low (190 ppmv) pCO_2 treatment and between 645 and 800 ppm for the high (750 ppmv) pCO_2 treatment (Fig. 2B). Based on these experiments it was decided to perform the second experimental series up to a cell concentration of circa $3.5*10^5$ cells mL^{-1} (dotted line in Fig. 2B).

3.2. Responses to different pCO_2 and irradiance regimes

Specific growth rate strongly depended on irradiance conditions (Table 1). Growth rates of *C. brevis* grown at growth-limiting irradiances (non-mixed 50 m and mixed 50 m) varied between 0.200 ± 0.003 day^{-1} (low CO_2, mixed 50 m) and 0.216 ± 0.001 day^{-1} (high CO_2, mixed 50 m)

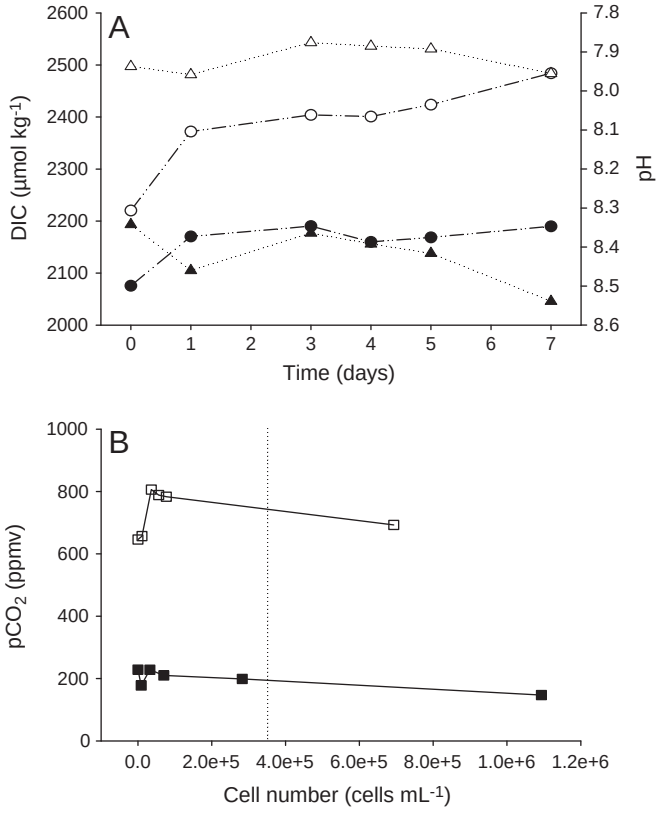

Fig. 2. Measured DIC (circles) and pH (triangles) (Fig. 2A) and calculated pCO_2 values (squares) vs cell numbers (Fig. 2B) in cultures of *Chaetoceros brevis* during the course of the initial experiments. The cultures were aerated with synthetic air containing 190 (low CO_2; closed symbols) or 750 (high CO_2; open symbols) ppmv CO_2. The dotted line in Fig. 2B represents the highest cell density in the second series of experiments ($3.5*10^5$ cells mL^{-1}, see text).

whereas growth rates at saturating irradiances (non-mixed 15 m and mixed 10 m) were higher, between 0.447 ± 0.008 day^{-1} (low CO_2, mixed 10 m) and 0.483 ± 0.001 day^{-1} (high CO_2, non-mixed 15 m). No significant effect of pCO_2 on growth could be demonstrated under these irradiance regimes (Table 1).

A range of photophysiological responses was observed between the four irradiance regimes (Table 1). In cultures grown at low constant irradiance (non-mixed 50 m) the average amount of light harvesting pigments (chlorophyll a + fucoxanthin) per cell was significantly higher while RuBisCO activity and E_k were significantly lower. Also RuBisCO expression was lower in these cultures. This effect was significant when compared to the "non-mixed 15 m" and the "mixed 10 m" treatments. Highest RuBisCO activity was measured in the cultures subjected to irradiance simulating shallow mixing (mixed 10 m), coinciding with highest P_{max} values. There were no significance differences in RuBisCO activity between the morning and noon samples (data not shown). The average amount of the photoprotective xanthophyll cycle pigments (diadinoxanthin + diatoxanthin) per cell was significantly higher in cultures that were exposed to short periods of high irradiance (mixed 50 m and mixed 10 m) compared to irradiance regimes simulating stable water column conditions. Particulate organic carbon (POC) cell quota varied between 8.55 ± 0.97 pg C $cell^{-1}$ and 13.0 ± 0.97 pg C $cell^{-1}$ and was significantly higher in cultures grown at non-fluctuating saturating irradiance (non-mixed 15 m). No significant differences ($p>0.05$) were found between the applied CO_2 conditions with respect to C:N ratio (data not shown), carbon and pigment content, photosynthetic parameters and RuBisCO activity and gene expression for all four irradiance regimes (Table 1).

De-epoxidation of diadinoxanthin to diatoxanthin was observed under all irradiance regimes except in the cultures that were grown at low constant irradiance (Fig. 3). The xanthophyll de-epoxidation state (EPS: the amount of the xanthophyll pigment diatoxanthin relative to the total xanthophyll cycle pigment pool) varied between 0 in the dark and 0.79 during the highest irradiance levels. A strong positive correlation ($r^2=0.92$) was observed between the EPS and photon flux density (PFD, data not shown) and between the cellular content of the xanthophyll pigment diatoxanthin and PFD (Fig. 4). Yet, the slope of this relationship was the same for both CO_2 treatments (0.051 and 0.052 [fg $cell^{-1}$] [µmol photons m^{-2} s^{-1}] $^{-1}$, for low and high pCO_2 respectively) indicating that xanthophyll cycling in *C. brevis* was not affected by pCO_2.

Highest values of effective quantum yield of photosynthesis Φ_{PSII} (F_v'/F_m') were recorded under the "non-mixed 50 m" regime (Fig. 3). There was a strong diel rhythm with decreasing values of Φ_{PSII} coinciding with increases in photon flux density (PFD). Again, there were no significant differences in EPS and Φ_{PSII} between CO_2 treatments.

4. Discussion

Our study demonstrates that neither elevated nor reduced CO_2 affects the performance of *C. brevis* under a range of semi-realistic photophysiological conditions. In contrast to CO_2, the irradiance regime strongly affected growth and physiology. In cultures grown at low constant irradiance the average amount of light harvesting pigments was significantly higher while the light saturation parameter E_k and the RuBisCO activity were significantly lower. Highest RuBisCO activity and maximum levels of photosynthetic activity (P_{max}) were measured in the "mixed 10 m" cultures which received the highest total daily light dose. In these cultures RuBisCO activity was comparable with levels previously measured in the temperate marine diatom *Thalassiosira weissflogii* exposed to natural levels of solar radiation (A.G.J. Buma, unpublished data). These results are consistent with other studies which showed that photosynthetic properties, RuBisCO content and maximal RuBisCO activity are

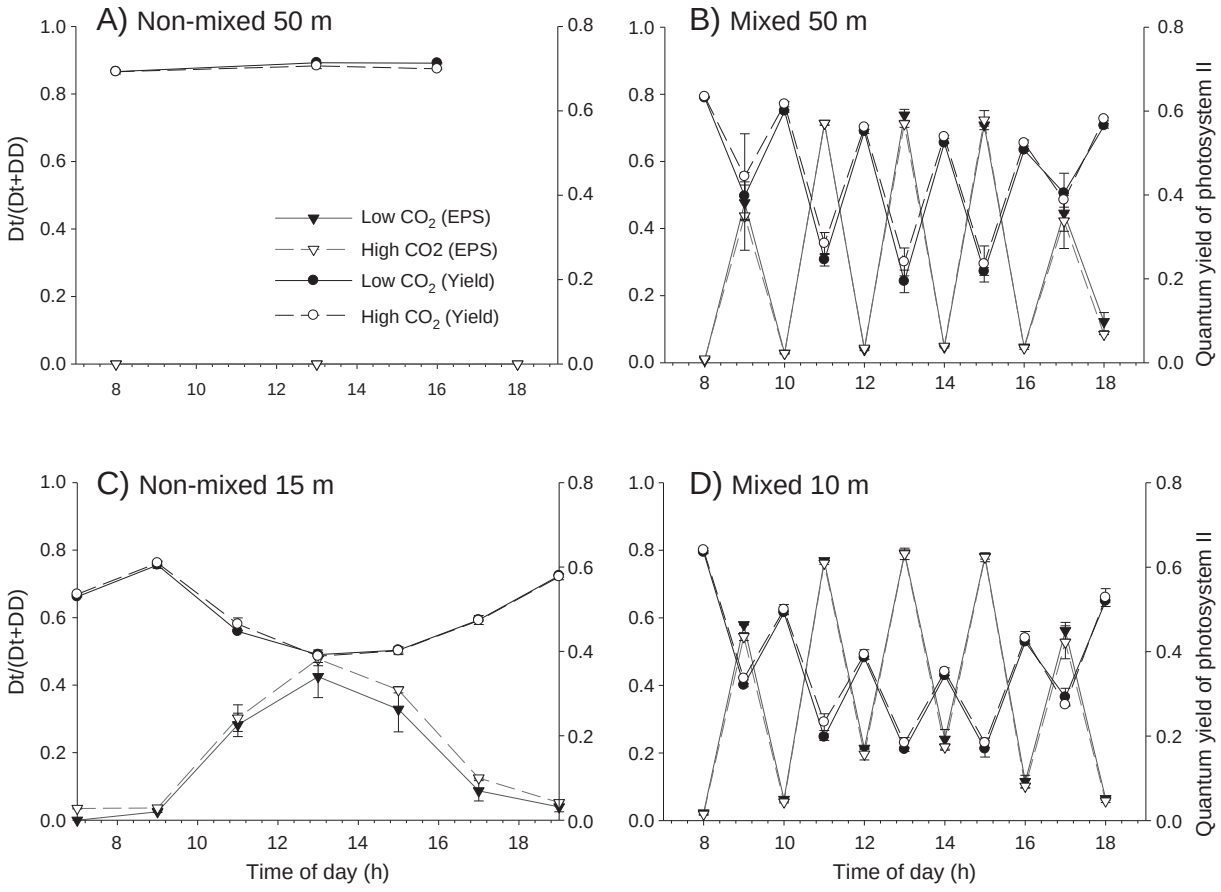

Fig. 3. The xanthophyll de-epoxidation state (EPS: the amount of the xanthophyll pigment diatoxanthin relative to the total xanthophyll pool) and effective quantum yield of photosynthesis Φ_{PSII} during the day of *Chaetoceros brevis* acclimated to high or low CO_2 and exposed to four different irradiance regimes. A) Growth-limiting low irradiance (non-mixed 50 m). B) Growth-limiting dynamic irradiance (mixed 50 m). C) Saturating irradiance (non-mixed 15 m). D) Saturating dynamic irradiance (mixed 10 m).

regulated in response to changes in irradiance (Rivkin, 1990; Orellana and Perry, 1992; Timmermans et al., 2001; van de Poll et al., 2005; Dubinsky and Stambler, 2009). Adjustment of cellular processes to low irradiance is an advantage in the Southern Ocean where irradiance levels can be low for a long period of time (e.g. during the winter or in areas covered with ice). In contrast, no significant differences in RuBisCO activity were found between the samples that were collected before 8:00 h (in the dark) and the noon samples,

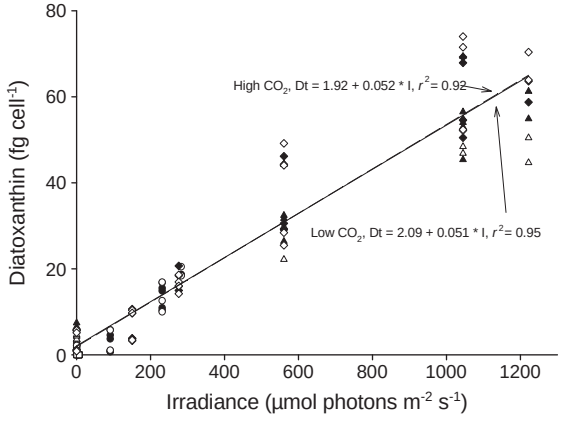

Fig. 4. Cellular content of the xanthophyll pigment diatoxanthin of *Chaetoceros brevis* acclimated to high or low CO_2 and exposed to four different irradiance regimes plotted against photon flux density (PFD). Non-mixed 50 m (circles); growth-limiting low irradiance. Mixed 50 m (triangles); growth-limiting dynamic irradiance. Non-mixed 15 m (squares); saturating irradiance. Mixed 10 m (diamonds); saturating dynamic irradiance. Closed symbols: low CO_2. Open symbols: high CO_2.

suggesting that regulation of RuBisCO activity in *C. brevis* is a process that operates on a longer than diurnal timescale. This also appears to be the case for the temperate phytoplankter *Emiliania huxleyi*. Harris et al. (2009) measured photoacclimation processes in *E. huxleyi* following shifts from low to high or high to low irradiance levels. They found that the cellular RuBisCO content did not change during at least the first 36 h after transition.

C. brevis rapidly deployed photoprotective mechanisms when exposed to occasional high levels of irradiance. Active xanthophyll cycling was observed under all irradiance regimes (except in the cultures that were grown at low constant light), which is consistent with other documented photoacclimation responses (Goss and Jakob, 2010). Xanthophyll cycle pigment pools (diadinoxanthin and diatoxanthin) were doubled under the light regimes that mimicked vertical mixing. A strong positive correlation was observed between the cellular content of the xanthophyll cycle pigment diatoxanthin and PFD, which allows maintenance of active photosystem II (PSII) in excessive PAR with a minimal requirement of energy-costly PSII repair mechanisms (van de Poll et al., 2006). Therefore, the activity of the xanthophyll cycle during the "mixed 10 m" conditions allowed *C. brevis* to grow with the same growth rate as that of the "non mixed 15 m" condition, showing the importance of this mechanism in minimizing PSII damage during high irradiance exposure. Xanthophyll cycle dynamics and effective quantum yield of photosynthesis (Φ_{PSII}) did not differ between high and low CO_2 conditions indicating that carboxylase activity was not limiting under any of the irradiance conditions.

Previous experiments by our group showed that *C. brevis*, like many other microalgae, has the ability to operate an efficient and regulated CCM (P. Boelen, unpublished results). Despite the extra

energetic costs needed to maintain a CCM, in our experiments no significant effects of pCO_2 on growth, photosynthetic performance and carboxylase activity were found under saturating as well as under limiting or dynamic irradiance conditions. Possibly, the energy consumed by the CCM is small compared to the total energy expended by *C. brevis*. Hopkinson et al. (2011) estimated the amount of energy used by the diatom *Phaeodactylum tricornutum* on its CCM and potential savings from CCM down regulation under high CO_2 conditions. They hypothesized that allocation of energetic savings to carbon fixation most likely occurs under conditions where growth is limited by energy generation, e.g. in light or nutrient limited environments. Under these conditions doubling of ambient CO_2 concentration would increase primary production by only a few percent. Our results agree with other studies on marine diatoms showing little or no effect of elevated pCO_2 on growth (Burkhardt et al., 1999) or maximum rates of photosynthesis (Rost et al., 2003; Trimborn et al., 2009). However, in other studies elevated CO_2 concentrations enhanced growth rates (e.g. Riebesell et al., 1993; Clark and Flynn, 2000) and reduced chlorophyll content (Sobrino et al., 2008). There have been only a few studies on the effect of changing pCO_2 on Antarctic diatoms so far. A recent field study in the Southern Ocean (Tortell et al., 2008) showed an increase in phytoplankton productivity and the promotion of large chain forming *Chaetoceros* species under elevated CO_2. Although no cell size data was collected in this study, cell sizes of the *Chaetoceros* spp. reported could be much larger than the small *C. brevis* (diameter circa 5 μm) we have used in our study. Since larger diatoms, with lower surface to volume ratios, may have a competitive disadvantage under low CO_2 conditions, it would be useful to compare size classes of *Chaetoceros* spp. in future studies. If the here observed negligible or absent effect of pCO_2 on growth is representative for Southern Ocean phytoplankton species, this would imply that other indirect effects of climate change have a stronger potential to influence Southern Ocean productivity. Our study suggests that changes in light regimes experienced by phytoplankton have a strong influence on productivity. Global change may reduce the depth of convective mixing in the Southern Ocean due to reduced surface density and salinity (Hirst, 1999). Such a change could increase phytoplankton light availability and probably enhance productivity. However, strong interactions can be expected with changes in trace metal availability (Wolff et al., 2006). Therefore future studies should concentrate on the interaction between these indirect effects of CO_2.

In conclusion, our study shows that the marine Antarctic diatom *C. brevis* can acclimate quickly to changing irradiance and pCO_2 conditions. This diatom can exploit irradiance regimes that include periods of excess irradiance (shallow vertical mixing and stable irradiance regimes). However, the regime mimicking deep vertical mixing clearly imposed limitations on growth. The results show that under saturating and limiting, as well as under dynamic and constant irradiance conditions the marine Antarctic diatom *C. brevis* has the ability to adjust its cellular physiology in response to changing pCO_2 levels with minimal effects on growth and photosynthesis.

Acknowledgements

We thank Astrid Hoogstraten, Jacqueline Stefels and Ronald J.W. Visser for constructive suggestions and technical support. This work was funded by the Dutch Council for Scientific Research (Dutch Polar Program grant number 851.20.031). **[SS]**

References

Alderkamp, A.C., de Baar, H.J.W., Visser, R.J.W., Arrigo, K.R., 2010. Can photoinhibition control phytoplankton abundance in deeply mixed water columns of the Southern Ocean? Limnol. Oceanogr. 55, 1248–1264.

Badger, M.R., Andrews, T.J., Whitney, S.M., Ludwig, M., Yellowlees, D.C., Leggat, W., Price, G.D., 1998. The diversity and coevolution of Rubisco, plastids, pyrenoids, and chloroplast-based CO_2-concentrating mechanisms in algae. Can. J. Bot.-Rev. Can. Bot. 76, 1052–1071.

Beardall, J., Giordano, M., 2002. Ecological implications of microalgal and cyanobacterial CO_2 concentrating mechanisms, and their regulation. Funct. Plant Biol. 29, 335–347.

Beardall, J., Raven, J.A., 2004. The potential effects of global climate change on microalgal photosynthesis, growth and ecology. Phycologia 43, 26–40.

Burkhardt, S., Riebesell, U., Zondervan, I., 1999. Effects of growth rate, CO_2 concentration, and cell size on the stable carbon isotope fractionation in marine phytoplankton. Geochim. Cosmochim. Acta 63, 3729–3741.

Clark, D.R., Flynn, K.J., 2000. The relationship between the dissolved inorganic carbon concentration and growth rate in marine phytoplankton. Proc. R. Soc. Lond. Ser. B-Biol. Sci. 267, 953–959.

Dickson, A.G., Millero, F.J., 1987. A comparison of the equilibrium-constants for the dissociation of carbonic-acid in seawater media. Deep-Sea Res. A-Oceanogr. Res. Pap. 34, 1733–1743.

DOE, 1994. Handbook of Methods for the Analysis of the Various Parameters of the Carbon Dioxide System in Sea Water; version 2. In: Dickson, A.G., Goyet, C. (Eds.), ORNL/CDIAC-74.

Dubinsky, Z., Stambler, N., 2009. Photoacclimation processes in phytoplankton: mechanisms, consequences, and applications. Aquat. Microb. Ecol. 56, 163–176.

Gerard, V.A., Driscoll, T., 1996. A spectrophotometric assay for rubisco activity: application to the kelp *Laminaria saccharina* and implications for radiometric assays. J. Phycol. 32, 880–884.

Goss, R., Jakob, T., 2010. Regulation and function of xanthophyll cycle-dependent photoprotection in algae. Photosynth. Res. 106, 103–122.

Guillard, R.R., Ryther, J.H., 1962. Studies of marine planktonic diatoms.1. *Cyclotella nana* Hustedt, and *Detonula confervacea* (Cleve) Gran. Can. J. Microbiol. 8, 229–239.

Harris, G.N., Scanlan, D.J., Geider, R.J., 2009. Responses of *Emiliania huxleyi* (Prymnesiophyceae) to step changes in photon flux density. Eur. J. Phycol. 44, 31–48.

Hirst, A.C., 1999. The Southern Ocean response to global warming in the CSIRO coupled ocean–atmosphere model. Environ. Model. Softw. 14 (4), 227–241.

Hopkinson, B.M., Dupont, C.L., Allen, A.E., Morel, F.M.M., 2011. Efficiency of the CO_2-concentrating mechanism of diatoms. Proc. Natl. Acad. Sci. U.S.A. 108 (10), 3830–3837. doi:10.1073/pnas.1018062108.

IPCC, 2007. Climate Change 2007: The Physical Science Basis. In: Solomon, S., Qin, D., Manning, M., et al. (Eds.), Contribution of Working Group I to the Fourth Assessment, Report of the Intergovernmental Panel on Climate Change. Cambridge University Press, Cambridge. United Kingdom and New York, NY, USA, 996 pp.

Lewis, E., Wallace, D.W.R., 1998. Program developed for CO_2 system calculations. ORNL/CDIAC-105. Carbon Dioxide Information Analysis Center, Oak Ridge National Laboratory, U.S. Department of Energy.

Livak, K.J., Schmittgen, T.D., 2001. Analysis of relative gene expression data using real-time quantitative PCR and the 2(T)(−Delta Delta C) method. Methods 25, 402–408.

MacIntyre, H.L., Kana, T.M., Geider, R.J., 2000. The effect of water motion on short-term rates of photosynthesis by marine phytoplankton. Trends Plant Sci. 5, 12–17.

Maxwell, K., Johnson, G.N., 2000. Chlorophyll fluorescence — a practical guide. J. Exp. Bot. 51, 659–668.

Mehrbach, C., Culberso, Ch., Hawley, J.E., Rm., Pytkowic, 1973. Measurement of apparent dissociation-constants of carbonic-acid in seawater at atmospheric-pressure. Limnol. Oceanogr. 18, 897–907.

Moisan, T.A., Olaizola, M., Mitchell, B.G., 1998. Xanthophyll cycling in *Phaeocystis antarctica*: changes in cellular fluorescence. Mar. Ecol. Prog. Ser. 169, 113–121.

Moore, C.M., Suggett, D.J., Hickman, A.E., Kim, Y.N., Tweddle, J.F., Sharples, J., Geider, R.J., Holligan, P.M., 2006. Phytoplankton photoacclimation and photoadaptation in response to environmental gradients in a shelf sea. Limnol. Oceanogr. 51, 936–949.

Nelson, D.M., Smith, W.O., 1991. Sverdrup revisited — critical depths, maximum chlorophyll levels, and the control of Southern-Ocean productivity by the irradiance-mixing regime. Limnol. Oceanogr. 36, 1650–1661.

Olaizola, M., Laroche, J., Kolber, Z., Falkowski, P.G., 1994. Nonphotochemical fluorescence quenching and the diadinoxanthin cycle in a marine diatom. Photosynth. Res. 41, 357–370.

Orellana, M.V., Perry, M.J., 1992. An immunoprobe to measure Rubisco concentrations and maximal photosynthetic rates of individual phytoplankton cells. Limnol. Oceanogr. 37, 478–490.

Ramakers, C., Ruijter, J.M., Deprez, R.H.L., Moorman, A.F.M., 2003. Assumption-free analysis of quantitative real-time polymerase chain reaction (PCR) data. Neurosci. Lett. 339, 62–66.

Reinfelder, J.R., 2011. Carbon concentrating mechanisms in eukaryotic marine phytoplankton. Annu. Rev. Mar. Sci. 3, 291–315.

Riebesell, U., Wolfgladrow, D.A., Smetacek, V., 1993. Carbon-dioxide limitation of marine-phytoplankton growth-rates. Nature 361, 249–251.

Rivkin, R.B., 1990. Photoadaptation in marine-phytoplankton — variations in ribulose 1,5-bisphosphate activity. Mar. Ecol. Prog. Ser. 62, 61–72.

Rost, B., Riebesell, U., Burkhardt, S., Sultemeyer, D., 2003. Carbon acquisition of bloom-forming marine phytoplankton. Limnol. Oceanogr. 48, 55–67.

Rozen, S., Skaletsky, H.J., 2000. Primer3 on the WWW for general users and for biologist programmers. In: Krawetz, S., Misener, S. (Eds.), Bioinformatics Methods and Protocols: Methods in Molecular Biology. Humana Press, Totowa, NJ, pp. 365–386.

Sakshaug, E., Slagstad, D., Holmhansen, O., 1991. Factors controlling the development of phytoplankton blooms in the Antarctic Ocean — a mathematical-model. Mar. Chem. 35, 259–271.

Sobrino, C., Ward, M.L., Neale, P.J., 2008. Acclimation to elevated carbon dioxide and ultraviolet radiation in the diatom *Thalassiosira pseudonana*: effects on growth, photosynthesis, and spectral sensitivity of photoinhibition. Limnol. Oceanogr. 53, 494–505.

Timmermans, K.R., Davey, M.S., van der Wagt, B., Snoek, J., Geider, R.J., Veldhuis, M.J.W., Gerringa, L.J.A., de Baar, H.J.W., 2001. Co-limitation by iron and light of *Chaetoceros brevis*, *C. dichaeta* and *C. calcitrans* (Bacillariophyceae). Mar. Ecol. Prog. Ser. 217, 287–297.

Tortell, P.D., Rau, G.H., Morel, F.M.M., 2000. Inorganic carbon acquisition in coastal Pacific phytoplankton communities. Limnol. Oceanogr. 45, 1485–1500.

Tortell, P.D., Payne, C.D., Li, Y.Y., Trimborn, S., Rost, B., Smith, W.O., Riesselman, C., Dunbar, R.B., Sedwick, P., DiTullio, G.R., 2008. CO_2 sensitivity of Southern Ocean phytoplankton. Geophys. Res. Lett. 35.

Trimborn, S., Wolf-Gladrow, D., Richter, K.U., Rost, B., 2009. The effect of pCO(2) on carbon acquisition and intracellular assimilation in four marine diatoms. J. Exp. Mar. Biol. Ecol. 376, 26–36.

van de Poll, W.H., Buma, A.G.J., 2009. Does ultraviolet radiation affect the xanthophyll cycle in marine phytoplankton? Photochem. Photobiol. Sci. 8, 1295–1301.

van de Poll, W.H., van Leeuwe, M.A., Roggeveld, J., Buma, A.G.J., 2005. Nutrient limitation and high irradiance acclimation reduce PAR and UV-induced viability loss in the Antarctic diatom *Chaetoceros brevis* (Bacillariophyceae). J. Phycol. 41, 840–850.

van de Poll, W.H., Alderkamp, A.C., Janknegt, P.J., Roggeveld, J., Buma, A.G.J., 2006. Photoacclimation modulates excessive photosynthetically active and ultraviolet radiation effects in a temperate and an Antarctic marine diatom. Limnol. Oceanogr. 51, 1239–1248.

van de Poll, W.H., Visser, R.J.W., Buma, A.G.J., 2007. Acclimation to a dynamic irradiance regime changes excessive irradiance sensitivity of *Emiliania huxleyi* and *Thalassiosira weissflogii*. Limnol. Oceanogr. 52, 1430–1438.

van Leeuwe, M.A., Villerius, L.A., Roggeveld, J., Visser, R.J.W., Stefels, J., 2006. An optimized method for automated analysis of algal pigments by HPLC. Mar. Chem. 102, 267–275.

Webb, W.L., Newton, M., Starr, D., 1974. Carbon-dioxide exchange of *Alnus rubra*—mathematical-model. Oecologia 17, 281–291.

Wolff, E.W., Fischer, H., Fundel, F., Ruth, U., Twarloh, B., Littot, G.C., Mulvaney, R., Roethlisberger, R., de Angelis, M., Boutron, C.F., Hansson, M., Jonsell, U., Hutterli, M.A., Lambert, F., Kaufmann, P., Stauffer, B., Stocker, T.F., Steffensen, J.P., Bigler, M., Siggaard-Andersen, M.L., Udisti, R., Becagli, S., Castellano, E., Severi, M., Wagenbach, D., Barbante, C., Gabrielli, P., Gaspari, V., 2006. Southern Ocean sea-ice extent, productivity and iron flux over the past eight glacial cycles. Nature 440, 491–496.